Supplemental Information

Figure S1, related to Figure 1

Breeding scheme used to produce the experimental cohorts.

5 alleles of *mTert, LSL-mTert*$^{L/L}$, *Pten*$^{L/L}$, *p53*$^{L/L}$, *PB-Cre4* were used to generate the telomere intact *mTert PB-Pten/p53* mice, G3/4 telomere dysfunctional *mTert-null mice* , G3/4 telomerase reactivation on the backdrop of telomere dysfunctional *LSL-Tert* mice.

Figure S2, related to Figure 2

Aggressive spread of G3/4 *LSL-mTert PB-Pten/p53* prostate tumors to spinal bones at 24 weeks of age. **(A)** H&E sections of the HPIN in the anterior prostate (AP) tumors at age of 9 weeks from G0 *mTert PB-Pten/p53 (*denoted as G0 *mTert*), G4 *mTert*$^{-/-}$ *PB-Pten/p53* **(**denoted as G4 *mTert*$^{-/-}$), and G4 *LSL-mTert PB-Pten/p53* **(**denoted as G4 *LSL-mTert*). **(B)** Prostate tumor cells from the primary sites and from spinal bones of G4 LSL-*Tert PB-Pten/p53* mouse at 24 weeks of age. (**C**) Prostate tumor cells from spinal bones of G4 LSL-*Tert PB-Pten/p53* mouse were micro-dissected, and the purified genomic DNA was used to detect the genomic status of floxed Pten by PCR **(D)**.

Figure S3, related to Figure 3

Telomere reserves were significantly increased in the G4 *LSL-mTert PB-Pten/p53* sample relative to G3/4 *mTert*$^{-/-}$ *PB-Pten/p53* prostate tumor.

(A) Representative telomere fluorescence *in situ* hybridization (FISH) of prostate tumors shows severe telomere erosion in G3/4 *mTert*$^{-/-}$ *PB-Pten/p53* cells (panel b), compared to G0 *mTert PB-Pten/p53* cells (panel a). Telomeres of G4 LSL-*Tert* cells were significantly maintained (panel c), compared to G3/4 *mTert*$^{-/-}$ *PB-Pten/p53* cells. **(B)** Relative telomere length in prostate tumors. Error bars represent s.d. for at least 4 to 6 independent measurements for each genotype.

Figure S4, related to Figure 4.

Genomic alterations in both mouse and human prostate tumor cells and derivation of 113 (37 amp and 76 del) genes correlated with bone metastasis.

There are a total of 94 MCRs in the aCGH dataset of G3/ G4 LSL-*Tert* prostate tumors (n=18). There are 741 genes (300 amp and 441 del) having the same genomic alteration pattern of amplification or deletion between the mouse prostate tumor dataset and Taylor *et al* (2010) human prostate cancer dataset (n=194). Among these 741 genes, there are a total of 228 genes (77 amp and 151 del) shown to be correlated with prostate cancer progression. Among these 228 genes, there are a total of 113 (37 amp and 76 del) genes shown to be correlated with bone metastasis.

Figure S5, related to Figure 5

Prognostic potential of a 14-gene set of bone metastatic tumor-enriched genes.

(A) Pathway enrichment analysis of bone metastasis of 113 gene set. P values were adjusted by false discovery rate (FDR). Enrichment of TGF-beta signaling pathway was highlighted by arrows. **(B)** The 14-gene set of ATP5A1/ATP6V1C1/CUL2/CYC1/DCC/ERCC3/MBD2/MTERF/PARD3/PTK2/RBL2/ SMAD2/SMAD4/SMAD7 can dichotomize PCA cases for BCR in Taylor et al data set (2010). **(C)** The 4-gene set of PTEN/SMAD4/CCND1/SPP1 can dichotomize PCA cases for BCR. **(D)** The combination of the 14-gene and PTEN/SMAD4/CCND1/SPP1 gene sets increases the predictive power of either gene set alone.

Table S1, related to Figure 2

Murine prostate cancer model used in this study.

Table S2, related to Figure 4

Significant copy number alterations (741 genes overlap with human PCA indicated on the right).

Table S3, related to Figure 4

The list of 77 amplified genes are related to metastatic phenotypes in any of the 6 databases, and 151 deleted genes are related to indolent phenotypes in any of the 6 Oncomine databases. AMP, gene amplification; DEL, gene deletion; BM, bone metastasis.

Table S4, related to Figure 5

Pathway enrichment analysis of bone metastasis of 113 gene set. P values were adjusted by false discovery rate (FDR).

Supplemental Figure

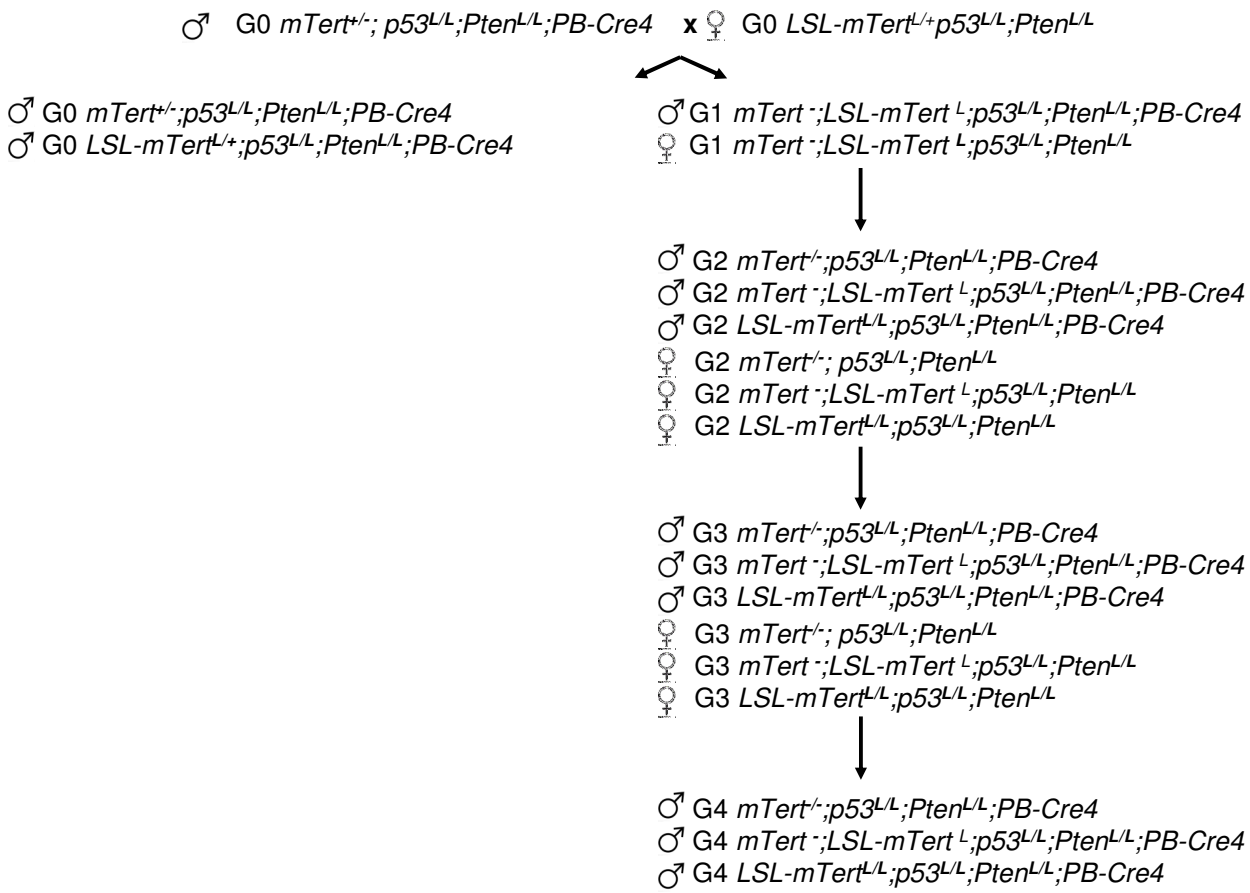

Ding et al. **Figure S1**

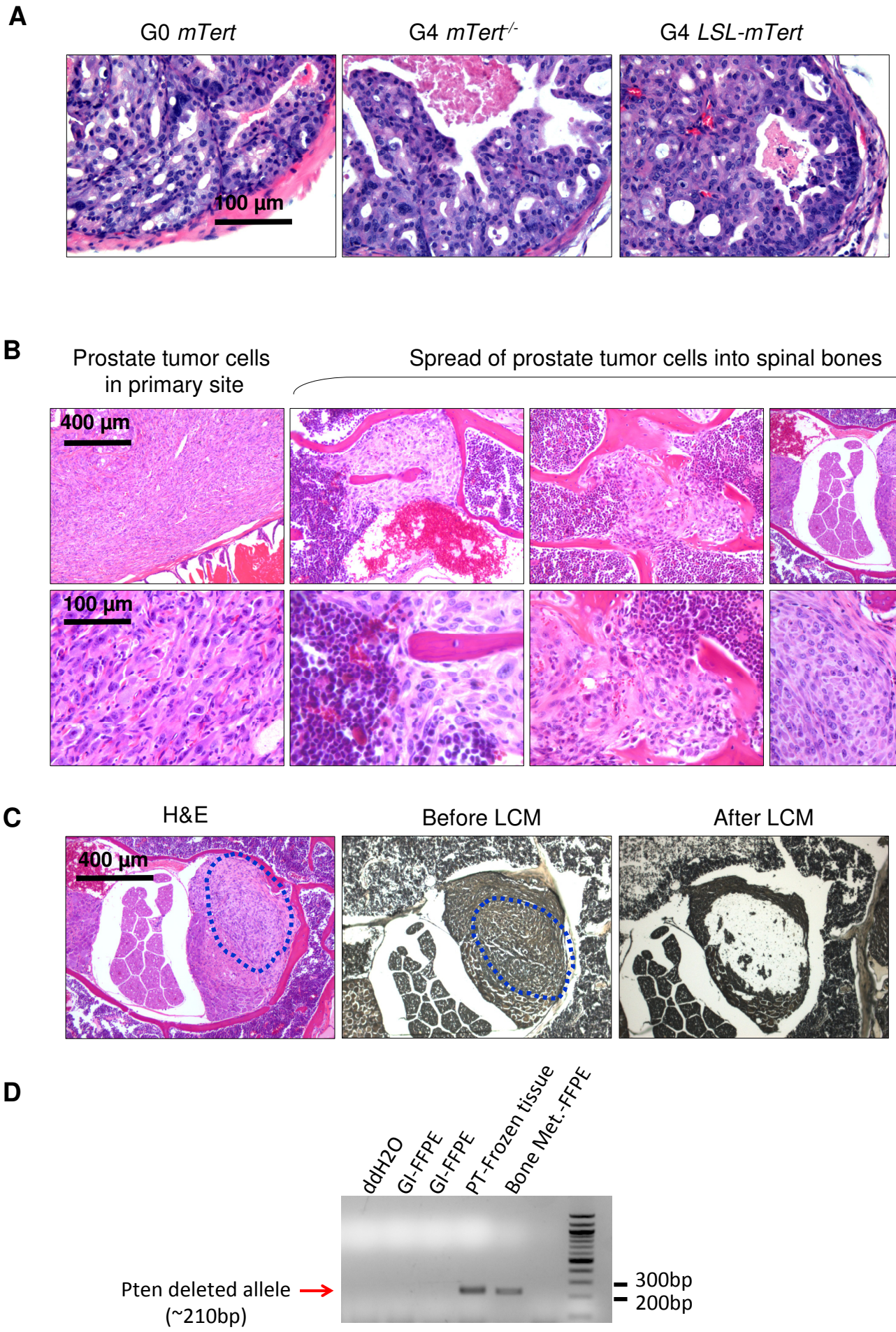

Ding et al. **Figure S2**

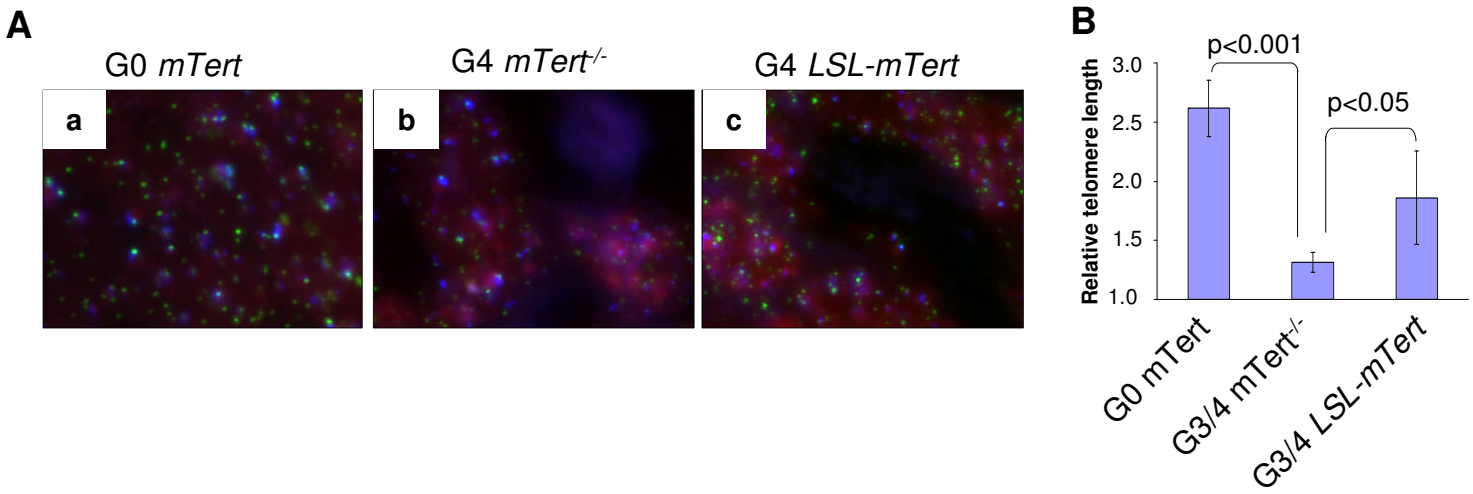

Ding et al. **Figure S3**

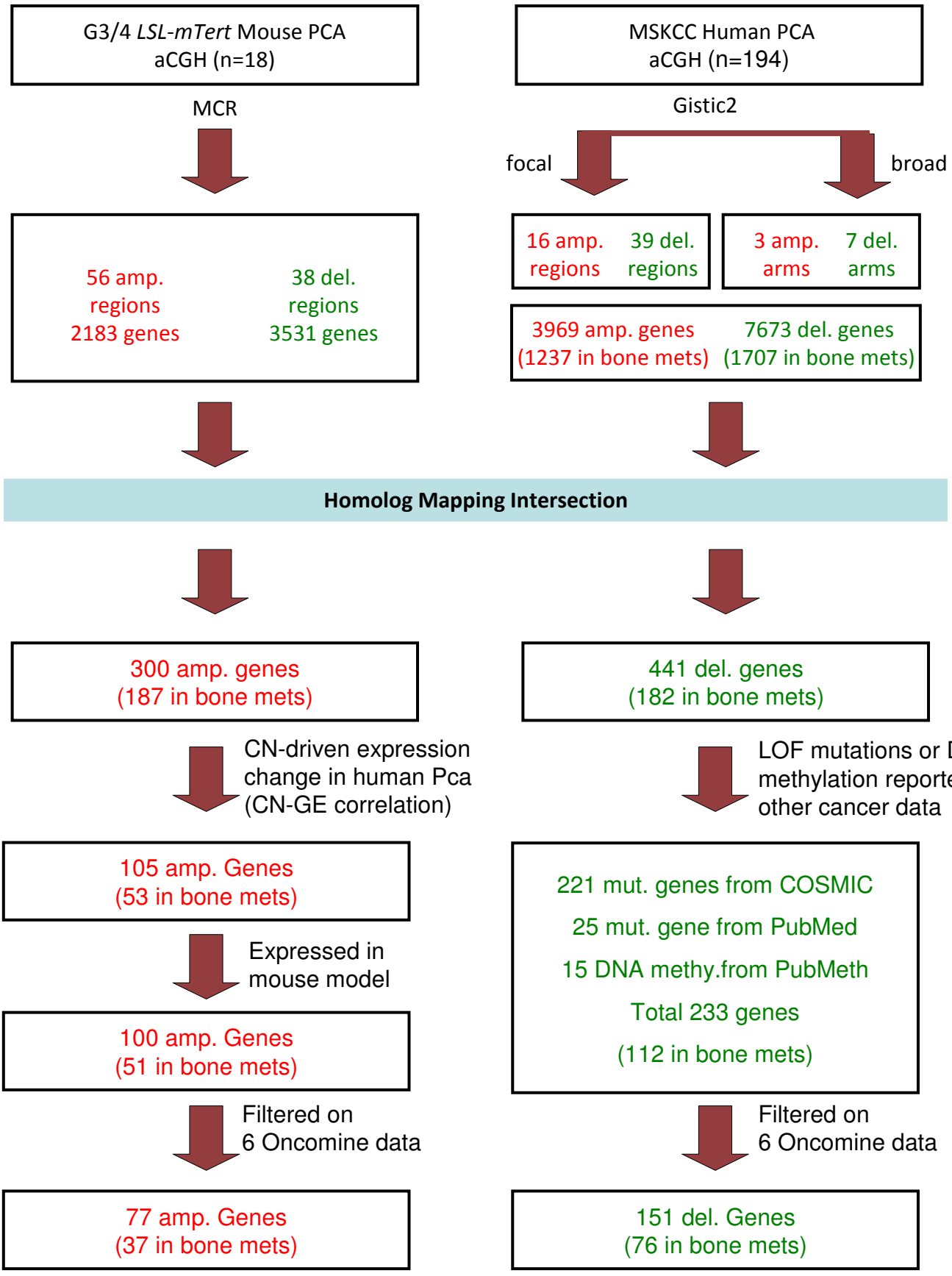

Ding et al. **Figure S4**

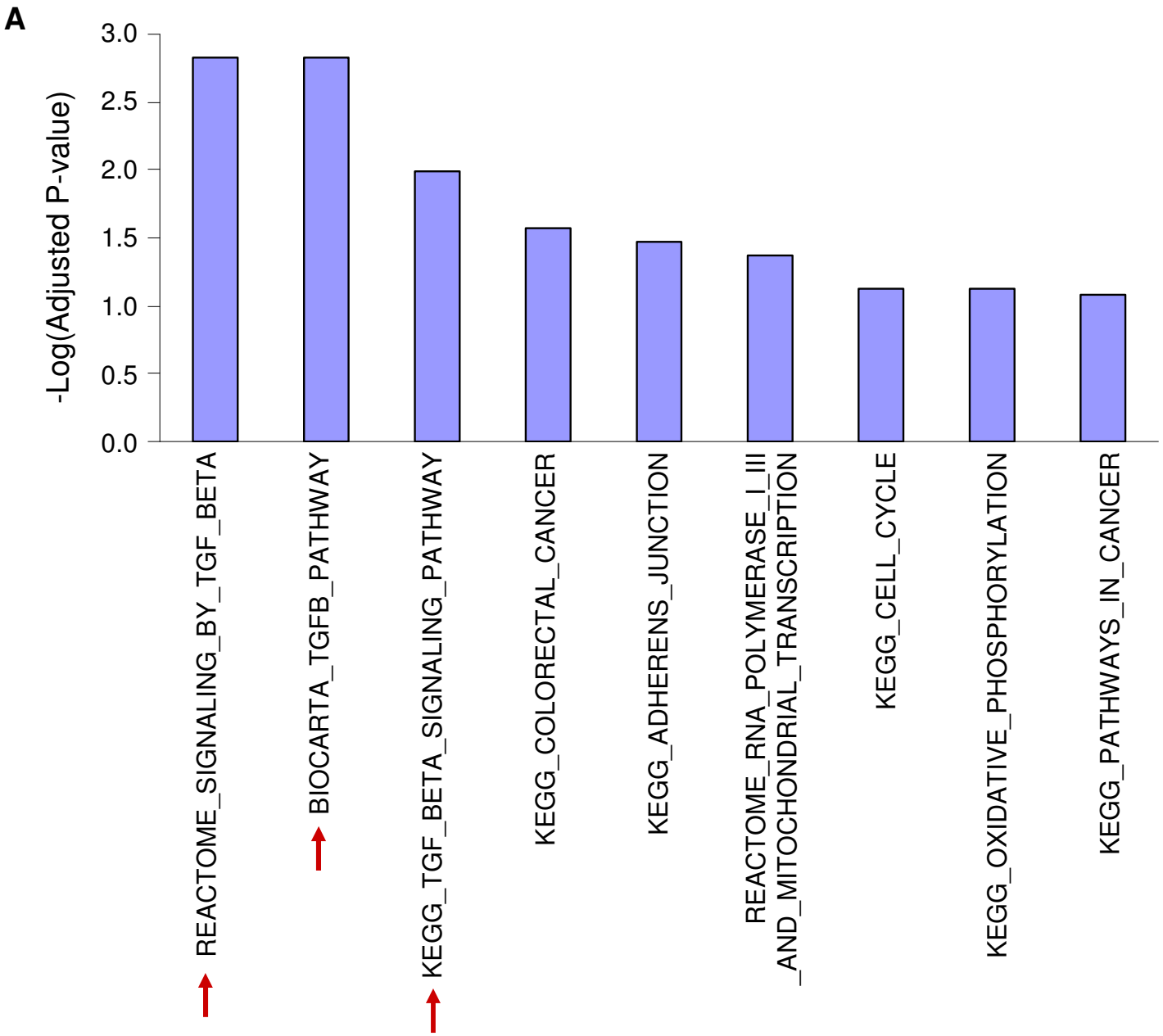

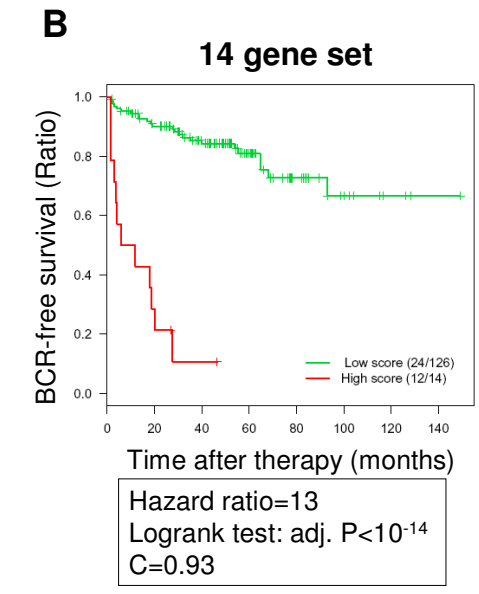

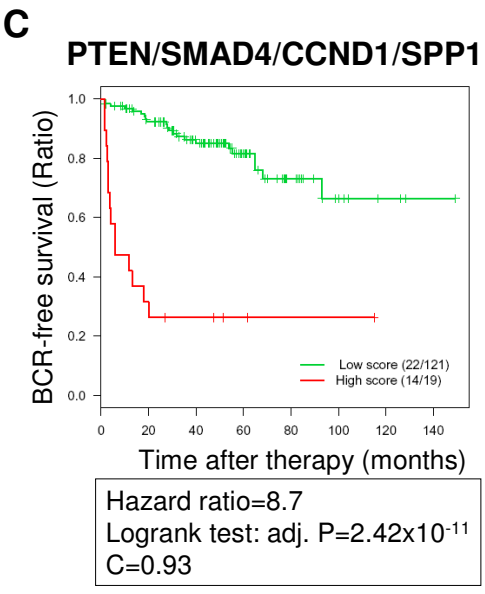

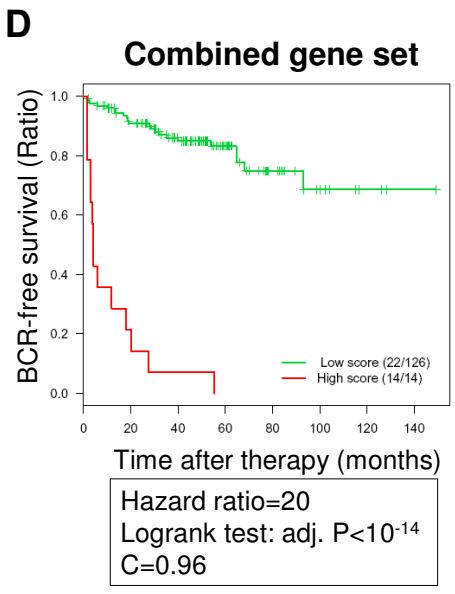

Ding et al. ***Supplemental*** **Fig. S5**